



---

*Research article*

## Stability switch and Hopf bifurcations for a diffusive plankton system with nonlocal competition and toxic effect

Liye Wang, Wenlong Wang\* and Ruizhi Yang

Department of Mathematics, Northeast Forestry University, Harbin 150040, China

\* **Correspondence:** Email: [wwl@nefu.edu.cn](mailto:wwl@nefu.edu.cn); Tel: +8613069720411.

**Abstract:** Since the distribution of plankton is always uneven, the nonlocal phytoplankton competition term indicates the spatial weighted mean of phytoplankton density, which is introduced into the plankton model with toxic substances effect to study the corresponding dynamic behavior. The stability of the positive equilibrium point and the existence of Hopf bifurcations are discussed by analysing the distribution of eigenvalues. The direction and stability of bifurcation periodic solution are researched based on an extended central manifold method and normal theory. Finally, spatially inhomogeneous oscillations are observed in the vicinity of the Hopf bifurcations. Through numerical simulation, we can observe that the system without nonlocal competition term only generates homogeneous periodic solution, and inhomogeneous periodic solution will produce only when both diffusion and nonlocal competition exist simultaneously. We can also see that when the toxin-producing rate of each phytoplankton is in an appropriate range, the system with nonlocal competition generates a stability switch with inhomogeneous periodic solution, when the value of time delay is in a certain interval, then Hopf bifurcations will appear, and with the increase of time delay, the quantity of plankton will eventually become stable.

**Keywords:** plankton; nonlocal competition; diffusion; delay; Hopf bifurcation

**Mathematics Subject Classification:** 34K18, 35B32

---

### 1. Introduction

Plankton is thought to be the basis of the oceanic food chain. Plankton, which is mainly composed of phytoplankton and zooplankton [1]. Zooplankton, like phytoplankton, is an indispensable natural feed for fish. Among them, phytoplankton has a positive impact on the water environment, but some species of phytoplankton have toxic effects on fish. Moreover, though Plankton is small in volume, is abundant in quantity and widely distributed, is the most important part of energy flow and material circulation in marine ecosystem. Its research has had a major impact on fisheries production and the

basic theory of marine science.

There are many kinds of mathematical models for studying Marine plankton systems. For different research purposes, they are different in the number of occurrence groups and influencing factors. Chakraborty et al. showed that when toxic effect occurs, the distribution of nutrients and phytoplankton became spatially heterogeneous and led to different patterns, with the distribution of nutrients and phytoplankton exhibiting spatial and temporal oscillations at certain levels of toxicity [2]. Meng found that imprecise parameters affect not only the internal and biological equilibrium of the system, but also the critical value of bifurcation and branching range [3]. Zhang engaged in the research of nontoxic phytoplankton, toxic phytoplankton, and zooplankton model [4]. In addition, the nutrient-phytoplankton-zooplankton model [5, 6] and nutrient-phytoplankton [7, 8] are also the research direction of many scholars.

Due to the widespread existence of time delays in nature, many scholars have studied population models with time delays [9–11]. The following plankton model with discrete delay was written out by Chattopadhyay and Sarkar [12],

$$\begin{cases} \frac{dP}{dt} = rP\left(1 - \frac{P}{K}\right) - \alpha PZ, \\ \frac{dZ}{dt} = \beta PZ - \mu Z - \frac{\theta P(t-\tau)Z}{\gamma + P(t-\tau)}. \end{cases} \quad (1.1)$$

All parameters are positive. Where  $P$  and  $Z$  represent the population density of phytoplankton and zooplankton, respectively.  $\alpha$  is the rate of specific predation and  $\beta$  describes the ratio of biomass consumed per zooplankton for the production of new zooplankton.  $\mu$  means zooplankton's mortality rate,  $\theta$  represents the rate of toxin production per phytoplankton species,  $\gamma$  denotes the half saturation constant and  $\tau$  is the discrete delay.

In [13], the diffusion term was added to the model(1.1) by Zhao J and Wei J, that is

$$\begin{cases} \frac{\partial P}{\partial t} = d_1 \Delta P + rP\left(1 - \frac{P}{K}\right) - \alpha PZ, \\ \frac{\partial Z}{\partial t} = d_2 \Delta Z + \beta PZ - \mu Z - \frac{\theta P(t-\tau)Z}{\gamma + P(t-\tau)}. \end{cases} \quad (1.2)$$

Where  $d_1$  and  $d_2$  are diffusion coefficients of phytoplankton and zooplankton, respectively. They mainly studied the dynamical behavior of models (1.2) with diffusion and delay.

Britton [14] and Furter and Greenfeld [15] proposed that the consumption of spatial place resources depends on two factors: the local population density and the weighted average population of the neighborhood. Because phytoplankton and zooplankton interact not only in the same location, but also in different locations, even in the whole space. With limited resources, there must be competition between phytoplankton and zooplankton. And most of the intraspecific and interspecific competitions for shared resources among individuals of mobile species are nonlocal. Therefore, it is necessary to introduce nonlocal competitive term into the dynamic model.

In recent years, nonlocal competition has also become the research object of many researchers. A diffusive predator-prey system with nonlocal intraspecific competition for prey was discussed by Geng, and they stated that from a biological perspective, global intraspecific competition promotes prey and predator coexistence by keeping prey at a critical total population size [16]. Pal et al. explored the 2D predator-prey model with nonlocal intraspecific competition, they showed that the bifurcation structure of the system is not as sensitive to the selection of parameterization as the relevant nonspatial case, which indicates that nonlocality likely reduce the structural sensitiveness of the system [17]. In [18],

Pal et al. also researched the effect of nonlocal competition on plankton-fish dynamics and showed the significance of non-locality in aquatic ecosystems and its possible contribution to the phenomena of spatial patchiness. There are also many other excellent models with nonlocal competition learned by researchers (see details to [19–21]). In [22], it showed that the most explicit way to introduce nonlocal effects is to replace  $\frac{u}{K}$  with  $\frac{\hat{u}(x,t)}{K}$ , where  $\hat{u}(x,t) = \int_{\Omega} G(x,y)u(y,t)dy$ . In this way, system (1.2) can be transformed into the following model

$$\begin{cases} \frac{\partial P(x,t)}{\partial t} = d_1 \Delta P(x,t) + rP(x,t) \left( 1 - \frac{1}{K} \int_{\Omega} G(x,y)P(y,t)dy \right) - \alpha P(x,t)Z(x,t), \\ \frac{\partial Z(x,t)}{\partial t} = d_2 \Delta Z(x,t) + \beta P(x,t)Z(x,t) - \mu Z(x,t) - \frac{\theta P(x,t-\tau)Z(x,t)}{\gamma + P(x,t-\tau)}, \quad x \in \Omega, t > 0, \\ \frac{\partial P(x,t)}{\partial \bar{\nu}} = \frac{\partial Z(x,t)}{\partial \bar{\nu}} = 0, \quad x \in \partial\Omega, t > 0, \\ P(x,\theta) = P_0(x,\theta) \geq 0, Z(x,\theta) = Z_0(x,\theta) \geq 0, \quad x \in \bar{\Omega}, \theta \in [-\tau, 0]. \end{cases} \quad (1.3)$$

Where  $\hat{P}(x,t) = \int_{\Omega} G(x,y)P(y,t)dy$  signifies the nonlocal phytoplankton competition effect. In order to make the calculation easier, we choose to study the eigenvalue problem in the one-dimensional space domain  $\Omega = (0, l\pi)$ , and  $G(x,y) = \frac{1}{l\pi}$  is the kernel function.

Although many scholars have studied the stability analysis and Hopf bifurcation of various models, stability analysis and Hopf bifurcation theory have also been widely used. In real life, the phenomenon of periodic oscillation is very normal, stability analysis of ecosystem behavior can allow us to come up with different ways to manage resources, and maintain a predictable state. So it is very necessary to study Hopf bifurcation and stability. In this paper, we also study them, with Hopf bifurcation as the main research content.

The layout design of this paper is as follows. In Section 2, we analyze the steady state condition of the positive equilibrium point and the existence of the Hopf bifurcations. In Section 3, we study the nature of Hopf bifurcation. In Section 4, to display the theoretical conclusions, we select appropriate parameters for numerical simulation. In Section 5, we come to a brief conclusion.

## 2. Stability analysis

It goes without saying that system (1.3) has two boundary equilibrium points  $(0, 0)$  and  $(K, 0)$ . Put forward the following hypothesis

$$(\mathbf{H}_0) \quad \theta < (\beta K - \mu) \left( 1 + \frac{\gamma}{K} \right).$$

Under the sufficient condition  $(\mathbf{H}_0)$ , the system (1.3) has an unique coexistence equilibrium point  $E_*(P_*, Z_*)$ , where

$$P_* = \frac{-(\beta\gamma - \mu - \theta) + \sqrt{(\beta\gamma - \mu - \theta)^2 + 4\beta\gamma\mu}}{2\beta}, \quad Z_* = \frac{r}{\alpha} \left( 1 - \frac{P_*}{K} \right).$$

Linearize system (1.3) at  $E_*(P_*, Z_*)$

$$\frac{\partial}{\partial t} \begin{pmatrix} P(x,t) \\ Z(x,t) \end{pmatrix} = D \begin{pmatrix} \Delta P(t) \\ \Delta Z(t) \end{pmatrix} + L_1 \begin{pmatrix} P(x,t) \\ Z(x,t) \end{pmatrix} + L_2 \begin{pmatrix} P(x,t-\tau) \\ Z(x,t-\tau) \end{pmatrix} + L_3 \begin{pmatrix} \hat{P}(x,t) \\ \hat{Z}(x,t) \end{pmatrix}, \quad (2.1)$$

where

$$D = \begin{pmatrix} d_1 & 0 \\ 0 & d_2 \end{pmatrix}, \quad L_1 = \begin{pmatrix} 0 & a_1 \\ a_2 & 0 \end{pmatrix}, \quad L_2 = \begin{pmatrix} 0 & 0 \\ b & 0 \end{pmatrix}, \quad L_3 = \begin{pmatrix} \hat{a} & 0 \\ 0 & 0 \end{pmatrix},$$

$$a_1 = -\alpha P_* < 0, \quad a_2 = \beta Z_* > 0, \quad b = \frac{-\gamma\theta Z_*}{(P_* + \gamma)^2} < 0, \quad \hat{a} = -\frac{rP_*}{K} < 0, \quad (2.2)$$

and  $\hat{P}(x, t) = \frac{1}{l\pi} \int_0^{l\pi} P(y, t) dy$ . After calculation, we can get the characteristic equations are

$$\lambda^2 + A_n \lambda + B_n - a_1 b e^{-\lambda \tau} = 0, \quad n \in \mathbb{N}, \quad (2.3)$$

where

$$A_0 = -\hat{a} > 0, \quad B_0 = -a_1 a_2 > 0,$$

$$A_n = (d_1 + d_2) \frac{n^2}{l^2} > 0, \quad B_n = d_1 d_2 \frac{n^4}{l^4} - a_1 a_2 > 0, \quad n \in \mathbb{N}^*. \quad (2.4)$$

Put forward the following assumption

$$(\mathbf{H}_1) \quad -a_1 a_2 - a_1 b > 0.$$

**Theorem 2.1.** *In system (1.3), if the assumption conditions  $\tau = 0$  and  $(\mathbf{H}_0)$  are contented. When  $(\mathbf{H}_1)$  is satisfied, then the coexistence equilibrium point  $E_*(P_*, Z_*)$  is locally asymptotically stable.*

*Proof.* When  $\tau = 0$ , the characteristic equation (2.3) of system (1.3) are

$$\lambda^2 - \hat{a} \lambda - a_1 a_2 - a_1 b = 0, \quad n = 0. \quad (2.5)$$

and

$$\lambda^2 + A_n \lambda + B_n - a_1 b = 0, \quad n \in \mathbb{N}^*, \quad (2.6)$$

When the term  $(\mathbf{H}_0)$  and  $(\mathbf{H}_1)$  are satisfied, we can conclude that the real part of the root of the characteristic equations (2.5) and (2.6) are negative, hence  $E_*(P_*, Z_*)$  is locally asymptotically stable.  $\square$

**Lemma 2.2.** *When  $(\mathbf{H}_0)$  and  $(\mathbf{H}_1)$  hold, Eq (2.3) has a pair of pure imaginary roots  $\pm i\omega_n^{\pm}$  at  $\tau_n^{j\pm}$ ,  $j \in \mathbb{N}$ ,  $n \in \mathbb{S}$ , where*

$$\omega_n^{\pm} = \sqrt{\frac{1}{2}[-(A_n^2 - 2B_n) \pm \sqrt{(A_n^2 - 2B_n)^2 - 4(B_n^2 - a_1^2 b^2)}]}, \quad (2.7)$$

and

$$\tau_n^{j\pm} = \frac{1}{\omega_n^{\pm}} \left[ 2\pi - \arccos\left(\frac{-\omega^2 + B_n}{a_1 b}\right) \right] + 2j\pi.$$

$$Z_{cos}^{(n)} = \frac{-\omega^2 + B_n}{a_1 b}, \quad Z_{sin}^{(n)} = \frac{-\omega A_n}{a_1 b} < 0, \quad (2.8)$$

$$\mathbb{S} = \{n | A_n^2 - 2B_n < 0, n \in \mathbb{N}\}.$$

*Proof.* Let  $i\omega$  ( $\omega > 0$ ) be a solution of Eq (2.3), then

$$-\omega^2 + i\omega A_n + B_n - a_1 b (\cos\omega\tau - i\sin\omega\tau) = 0.$$

$\cos\omega\tau = \frac{-\omega^2 + B_n}{a_1 b}$ ,  $\sin\omega\tau = \frac{-\omega A_n}{a_1 b}$  can be calculated easily. It leads to

$$\omega^4 + \omega^2 (A_n^2 - 2B_n) + B_n^2 - a_1^2 b^2 = 0. \quad (2.9)$$

Making  $z = \omega^2$ , hence the Eq (2.9) becomes

$$z^2 + z(A_n^2 - 2B_n) + B_n^2 - a_1^2 b^2 = 0, \quad (2.10)$$

and  $z^\pm = \frac{1}{2}[-(A_n^2 - 2B_n) \pm \sqrt{(A_n^2 - 2B_n)^2 - 4(B_n^2 - a_1^2 b^2)}]$  are the roots of Eq (2.10). There's no denying that when  $(\mathbf{H}_0)$  and  $(\mathbf{H}_1)$  are met, then  $B_n - a_1 b > 0$ ,  $B_n + a_1 b > 0$  for  $n \in \mathbb{N}$ . By accurate calculation, we can get  $A_0^2 - 2B_0 = \hat{a}^2 + 2a_1 a_2$ ,  $A_n^2 - 2B_n = d_1^2 \frac{n^4}{l^4} + d_2^2 \frac{n^4}{l^4} + 2a_1 a_2$ . Due to  $\lim_{n \rightarrow \infty} (A_n^2 - 2B_n) \rightarrow +\infty$ , obviously to see  $\mathbb{S}$  is a finite set. You can get  $z^+ > 0$  and  $z^- > 0$  for  $n \in \mathbb{S}$  obviously. Thus,  $\pm i\omega_n^\pm$  is a pair of purely imaginary roots of the Eq (2.3) at  $\tau_n^{j\pm}$ ,  $j \in \mathbb{N}$ ,  $n \in \mathbb{S}$ .  $\square$

**Lemma 2.3.** When  $(\mathbf{H}_0)$  and  $(\mathbf{H}_1)$  are contended, then  $\operatorname{Re}[\frac{d\lambda}{d\tau}|_{\tau=\tau_n^{j+}}] > 0$ ,  $\operatorname{Re}[\frac{d\lambda}{d\tau}|_{\tau=\tau_n^{j-}}] < 0$  for  $n \in \mathbb{S}$ ,  $j \in \mathbb{N}$ .

*Proof.* By Eq (2.3), we can get

$$\left(\frac{d\lambda}{d\tau}\right)^{-1} = \frac{2\lambda + A_n}{-a_1 b \lambda e^{-\lambda\tau}} - \frac{\tau}{\lambda}.$$

Then

$$\begin{aligned} \left[\operatorname{Re}\left(\frac{d\lambda}{d\tau}\right)^{-1}\right]_{\tau=\tau_n^{j\pm}} &= \operatorname{Re}\left[\frac{2\lambda + A_n}{-a_1 b \lambda e^{-\lambda\tau}} - \frac{\tau}{\lambda}\right]_{\tau=\tau_n^{j\pm}} \\ &= \left[\frac{1}{a_1^2 b^2} (A_n^2 - 2B_n + 2\omega^2)\right]_{\tau=\tau_n^{j\pm}} \\ &= \pm \left[\frac{1}{a_1^2 b^2} \sqrt{(A_n^2 - 2B_n)^2 + 4(B_n^2 - a_1^2 b^2)}\right]_{\tau=\tau_n^{j\pm}}. \end{aligned}$$

Therefore, we can get  $\operatorname{Re}[\frac{d\lambda}{d\tau}|_{\tau=\tau_n^{j+}}] > 0$ ,  $\operatorname{Re}[\frac{d\lambda}{d\tau}|_{\tau=\tau_n^{j-}}] < 0$  for  $n \in \mathbb{S}$ ,  $j \in \mathbb{N}$ .

Denote  $\tau_* = \min\{\tau_n^{0,\pm} | n \in \mathbb{S}\}$ ,  $\tau_{max} = \max\{\tau_n^{0,\pm} | n \in \mathbb{S}\}$ . According to the above results, we can get the following theorem.

**Theorem 2.4.** When  $(\mathbf{H}_0)$  and  $(\mathbf{H}_1)$  are satisfied, then the following expressions are correct for system (1.3):

- (1)  $E_*(P_*, Z_*)$  is locally asymptotically stable for  $\tau \in [0, \tau_*)$ .
- (2)  $E_*(P_*, Z_*)$  is unstable for  $\tau \in (\tau_*, \tau_* + \varepsilon)$  with some  $\varepsilon > 0$ .
- (3) At  $\tau = \tau_n^{j\pm}$  or  $\tau_n^{0,\pm}$  ( $n \in \mathbb{S}$ ,  $j \in \mathbb{N}$ ), system (1.3) underdoes Hopf bifurcation.

### 3. Property of Hopf bifurcation

The same method as [23, 24] is adopted by us to compute the Hopf bifurcations in detail. For fixed  $j \in \mathbb{N}$  and  $n \in \mathbb{S}$ , we definite  $\tilde{\tau} = \tau_n^{j\pm}$ . Make  $\tilde{P}(x, t) = P(x, \tau t) - P_*$  and  $\tilde{Z}(x, t) = Z(x, \tau t) - Z_*$ . Hence the system (1.3) can be transformed into(drop the tilde)

$$\begin{cases} \frac{\partial P}{\partial t} = \tau[d_1\Delta P + r(P + P_*)\left(1 - \frac{1}{Kl\pi} \int_0^{l\pi} (P(y, t) + P_*)dy\right) - \alpha(P + P_*)(Z + Z_*)], \\ \frac{\partial Z}{\partial t} = \tau[d_2\Delta Z + \beta(P + P_*)(Z + Z_*) - \mu(Z + Z_*) - \frac{\theta(P(t-1) + P_*)(Z + Z_*)}{\gamma + P(t-1) + P_*}]. \end{cases} \quad (3.1)$$

After simplification, the system (3.1) can be converted into

$$\begin{cases} \frac{\partial P}{\partial t} = \tau[d_1\Delta P + a_1Z + \hat{a}\hat{P} + \beta_1\hat{P}P + \beta_2PZ] + h.o.t., \\ \frac{\partial Z}{\partial t} = \tau[d_2\Delta Z + a_2P + bP(t-1) + \beta_3PZ + \beta_4P(t-1)Z + \beta_5P^2(t-1) \\ + \beta_6P^3(t-1) + \beta_7P^2(t-1)Z] + h.o.t., \end{cases} \quad (3.2)$$

where

$$\beta_1 = -\frac{r}{K}, \quad \beta_2 = -\alpha, \quad \beta_3 = \beta, \quad \beta_4 = -\frac{\gamma\theta}{(P_* + \gamma)^2},$$

$$\beta_5 = \frac{\gamma\theta Z_*}{(P_* + \gamma)^3}, \quad \beta_6 = -\frac{\gamma\theta Z_*}{(P_* + \gamma)^4}, \quad \beta_7 = \frac{\gamma\theta}{(P_* + \gamma)^3}.$$

Define a real-valued Sobolev space  $X := \{(P, Z)^T : P, Z \in H^2(0, l\pi), (P_x, Z_x)|_{x=0, l\pi} = 0\}$ , the complexification of  $X_{\mathbb{C}} := X \oplus iX = \{x_1 + ix_2 | x_1, x_2 \in X\}$ . And the inner product  $\langle \tilde{P}, \tilde{Z} \rangle := \int_0^{l\pi} \overline{P_1} Z_1 dx + \int_0^{l\pi} \overline{P_2} Z_2 dx$  for  $\tilde{P} = (P_1, P_2)^T$ ,  $\tilde{Z} = (Z_1, Z_2)^T$ ,  $\tilde{P}, \tilde{Z} \in X_{\mathbb{C}}$ ,  $\overline{P_1}$  and  $\overline{P_2}$  represent the conjugate of  $P_1$  and  $P_2$ , respectively. The phase space  $\mathcal{C} := C([-1, 0], X)$  has the sup norm, hence  $\phi_t \in \mathcal{C}$ ,  $\phi_t(\theta) = \phi(t + \theta)$  or  $-1 \leq \theta \leq 0$ . Denote  $\beta_n^{(1)}(x) = (\gamma_n(x), 0)^T$ ,  $\beta_n^{(2)}(x) = (0, \gamma_n(x))^T$ , and  $\beta_n = \{\beta_n^{(1)}(x), \beta_n^{(2)}(x)\}$ , where  $\{\beta_n^{(j)}(x)\}$  is an orthonormal basis of  $X$ . Let's define  $\mathbb{B}_n := \text{span}\{\langle \phi(\cdot), \beta_n^{(j)} \rangle \beta_n^{(j)} | \phi \in \mathcal{C}, j = 1, 2\}$ ,  $n \in \mathbb{N}_0$  as a subspace of  $\mathcal{C}$ . There exists a  $2 \times 2$  matrix function  $\eta^n(\sigma, \tilde{\tau}) - 1 \leq \sigma \leq 0$ , make  $-\tilde{\tau}D_{\tilde{\tau}}^2 \phi(0) + \tilde{\tau}L(\phi) = \int_{-1}^0 d\eta^n(\sigma, \tau)\phi(\sigma)$  for  $\phi \in \mathcal{C}$ . The bilinear form on  $\mathcal{C}^* \times \mathcal{C}$  is defined by

$$(\psi, \phi) = \psi(0)\phi(0) - \int_{-1}^0 \int_{\xi=0}^{\sigma} \psi(\xi - \sigma) d\eta^n(\sigma, \tilde{\tau}) \phi(\xi) d\xi, \quad (3.3)$$

for  $\phi \in \mathcal{C}$ ,  $\psi \in \mathcal{C}^*$ . Define  $\tau = \tilde{\tau} + \mu$ , when  $\mu = 0$ , then the system has a pair of purely imaginary roots  $\pm i\omega_{n_0}$  at  $(0, 0)$ , and undergoes Hopf bifurcation. The infinitesimal generator of a semigroup is represented as  $A$ , and the formal adjoint of  $A$  in bilinear form (3.3) is represented as  $A^*$ . Define the following function

$$\delta(n_0) = \begin{cases} 1 & n_0 = 0, \\ 0 & n_0 \in \mathbb{N}. \end{cases} \quad (3.4)$$

Choose  $\eta_{n_0}(0, \tilde{\tau}) = \tilde{\tau}[(-n_0^2/l^2)D + L_1 + L_3\delta(n_{n_0})]$ ,  $\eta_{n_0}(-1, \tilde{\tau}) = -\tilde{\tau}L_2$ ,  $\eta_{n_0}(\sigma, \tilde{\tau}) = 0$  for  $-1 < \sigma < 0$ . Let  $s(\theta) = s(0)e^{i\omega_{n_0}\tilde{\tau}\theta}$  ( $\theta \in [-1, 0]$ ),  $q(\vartheta) = q(0)e^{-i\omega_{n_0}\tilde{\tau}\vartheta}$  ( $\vartheta \in [0, 1]$ ) be the eigenfunctions of  $A(\tilde{\tau})$  and  $A^*$  corresponds to  $i\omega_{n_0}\tilde{\tau}$  respectively. We can make  $s(0) = (1, s_1)^T$ ,  $q(0) = M(1, q_2)$ , where  $s_1 = \frac{1}{a_1}(i\omega_{n_0} + d_1n_0^2/l^2 - \hat{a}\delta(n_0))$ ,  $q_2 = a_1l^2/(d_2n^2 + i\omega_{n_0}l^2)$ , and  $M = (1 + s_1q_2 + \tilde{\tau}q_2be^{-i\omega_{n_0}\tilde{\tau}})^{-1}$ . Then we rewrite (3.1) into the following system in an abstract form

$$\frac{dP(t)}{dt} = (\tilde{\tau} + \mu)D\Delta P(t) + (\tilde{\tau} + \mu)[L_1(P_t) + L_2P(t - 1) + L_3\hat{P}(t)] + F(P_t, \hat{P}_t, \mu), \tag{3.5}$$

where

$$F(\phi, \mu) = (\tilde{\tau} + \mu) \begin{pmatrix} \beta_1\phi_1(0)\hat{\phi}_1(0) + \beta_2\phi_1(0)\phi_2(0) \\ \beta_3\phi_1(0)\phi_2(0) + \beta_4\phi_1(-1)\phi_2(0) + \beta_5\phi_1^2(-1) + \beta_6\phi_1^3(-1) + \beta_7\phi_1^2(-1)\phi_2(0) \end{pmatrix} \tag{3.6}$$

respectively, for  $\phi = (\phi_1, \phi_2)^T \in \mathcal{C}$  and  $\hat{\phi}_1 = \frac{1}{l\pi} \int_0^{l\pi} \phi dx$ . Then the space  $\mathcal{C}$  can be decomposed as  $\mathcal{C} = S \oplus Q$ , where  $S = \{z s \gamma_{n_0}(x) + \bar{z} \bar{s} \gamma_{n_0}(x) | z \in \mathbb{C}\}$ ,  $Q = \{\phi \in \mathcal{C} | (q \gamma_{n_0}(x), \phi) = 0 \text{ and } (\bar{q} \gamma_{n_0}(x), \phi) = 0\}$ . Then, system (3.6) can be rewritten as  $P_t = z(t)s(\cdot)\gamma_{n_0}(x) + \bar{z}(t)\bar{s}(\cdot)\gamma_{n_0}(x) + \omega(t, \cdot)$  and  $\hat{P}_t = \frac{1}{l\pi} \int_0^{l\pi} P_t dx$ , where

$$z(t) = (q \gamma_{n_0}(x), P_t), \quad \omega(t, \theta) = P_t(\theta) - 2\text{Re}\{z(t)s(\theta)\gamma_{n_0}(x)\}. \tag{3.7}$$

then, we have  $\dot{z}(t) = i\omega_{n_0}\tilde{\tau}z(t) + \bar{q}(0) \langle F(0, P_t), \beta_{n_0} \rangle$ . There occurs a center manifold  $C_0$ , and near  $(0, 0)$ ,  $\omega$  can be written as follow.

$$\omega(t, \theta) = \omega(z(t), \bar{z}(t), \theta) = \omega_{20}(\theta)\frac{z^2}{2} + \omega_{11}(\theta)z\bar{z} + \omega_{02}(\theta)\frac{\bar{z}^2}{2} + \dots \tag{3.8}$$

Then, limiting the system to the central manifold becomes  $\dot{z}(t) = i\omega_{n_0}\tilde{\tau}z(t) + g(z, \bar{z})$ . Denote  $g(z, \bar{z}) = g_{20}\frac{z^2}{2} + g_{11}z\bar{z} + g_{02}\frac{\bar{z}^2}{2} + g_{21}\frac{z\bar{z}^2}{2} + \dots$ . And by exact calculation, we get

$$g_{20} = 2\tilde{\tau}M(\varsigma_1 + q_2\varsigma_2)I_3, \quad g_{11} = \tilde{\tau}M(\varrho_1 + q_2\varrho_2)I, \quad g_{02} = \bar{g}_{20},$$

$$g_{21} = 2\tilde{\tau}M[(\kappa_{11} + q_2\kappa_{21})I_3 + (\kappa_{12} + q_2\kappa_{22})I_4],$$

where  $I_3 = \int_0^{l\pi} \gamma_{n_0}^3(x)dx$ ,  $I_4 = \int_0^{l\pi} \gamma_{n_0}^4(x)dx$ ,  $\varsigma_1 = \beta_1\delta(n_0) + \beta_2s_1$ ,  $\varsigma_2 = e^{-2i\tilde{\tau}\omega_{n_0}}\beta_5 + \beta_3s_1 + e^{-i\tilde{\tau}\omega_{n_0}}\beta_4s_1$ ,  $\varrho_1 = \frac{1}{2}\beta_1\delta(n_0) + \frac{1}{4}\beta_2\bar{s}_1 + \frac{1}{4}\beta_2s_1$ ,  $\varrho_2 = \frac{1}{2}\beta_5 + \beta_3(\frac{1}{4}\bar{s}_1 + \frac{1}{4}s_1) + \beta_4(\frac{1}{4}e^{-i\tilde{\tau}\omega_{n_0}}\bar{s}_1 + \frac{1}{4}e^{-i\tilde{\tau}\omega_{n_0}}s_1)$ ,  $\kappa_{11} = \omega_{11}^{(1)}(0)(2\beta_1\delta(n_0) + 2\beta_1 + 2\beta_2s_1) + \omega_{20}^{(1)}(0)(\beta_1\delta(n_0) + \beta_1 + \beta_2\bar{s}_1) + 2\omega_{11}^{(2)}(0)\beta_2 + \omega_{20}^{(2)}(0)\beta_2$ ,  $\kappa_{12} = 0$ ,  $\kappa_{21} = \omega_{20}^{(1)}(0)\beta_3\bar{s}_1 + 2\omega_{11}^{(1)}(0)\beta_3s_1 + \omega_{11}^{(2)}(0)(2\beta_3 + 2\beta_4e^{-i\tilde{\tau}\omega_{n_0}}) + \omega_{20}^{(2)}(0)(\beta_3 + e^{i\tilde{\tau}\omega_{n_0}}\beta_4) + \omega_{20}^{(1)}(-1)(2\beta_5e^{i\tilde{\tau}\omega_{n_0}} + \beta_4\bar{s}_1) + \omega_{11}^{(1)}(-1)(4e^{-i\tilde{\tau}\omega_{n_0}}\beta_5 + 2\beta_4s_1)$ ,  $\kappa_{22} = \frac{3}{2}e^{-i\tilde{\tau}\omega_{n_0}}\beta_6 + \frac{1}{2}e^{-2i\tilde{\tau}\omega_{n_0}}\beta_7\bar{s}_1 + \beta_7s_1$ .

Now, we calculate  $W_{20}(\theta)$  and  $W_{11}(\theta)$  when  $n=0$ , and get  $g_{21}$ . By (3.7), we have

$$\dot{\omega} = \hat{P}_t - \dot{z}h\gamma_{n_0}(x) - \dot{\bar{z}}\bar{h}\gamma_{n_0}(x) = A\omega + H(z, \bar{z}, \theta), \tag{3.9}$$

where

$$H(z, \bar{z}, \theta) = H_{20}(\theta)\frac{z^2}{2} + H_{11}(\theta)z\bar{z} + H_{02}(\theta)\frac{\bar{z}^2}{2} + \dots \tag{3.10}$$

By comparing the coefficients of (3.8) and (3.9), we can obtain

$$(A - 2i\omega_{n_0}\tilde{\tau}I)\omega_{20} = -H_{20}(\theta), \quad A\omega_{11}(\theta) = -H_{11}(\theta). \tag{3.11}$$

Then, we can get

$$\begin{aligned}\omega_{20}(\theta) &= \frac{-g_{20}}{i\omega_{n_0}\tilde{\tau}}p(0)e^{i\omega_{n_0}\tilde{\tau}\theta} - \frac{\bar{g}_{02}}{3i\omega_{n_0}\tilde{\tau}}\bar{p}(0)e^{-i\omega_{n_0}\tilde{\tau}\theta} + E_1e^{2i\omega_{n_0}\tilde{\tau}\theta}, \\ \omega_{11}(\theta) &= \frac{g_{11}}{i\omega_{n_0}\tilde{\tau}}p(0)e^{i\omega_{n_0}\tilde{\tau}\theta} - \frac{\bar{g}_{11}}{i\omega_{n_0}\tilde{\tau}}\bar{p}(0)e^{-i\omega_{n_0}\tilde{\tau}\theta} + E_2,\end{aligned}\tag{3.12}$$

where  $E_1 = \sum_{n=0}^{\infty} E_1^{(n)}$ ,  $E_2 = \sum_{n=0}^{\infty} E_2^{(n)}$ ,

$$\begin{aligned}E_1^{(n)} &= (2i\omega_{n_0}\tilde{\tau}I - \int_{-1}^0 e^{2i\omega_{n_0}\tilde{\tau}\theta}d\eta_{n_0}(\theta, \tilde{\tau}))^{-1} \langle \tilde{F}_{20}, \beta_n \rangle, \\ E_2^{(n)} &= -(\int_{-1}^0 d\eta_{n_0}(\theta, \tilde{\tau}))^{-1} \langle \tilde{F}_{11}, \beta_n \rangle, \quad n \in \mathbb{N}_0,\end{aligned}$$

$$\langle \tilde{F}_{20}, \beta_n \rangle = \begin{cases} \frac{1}{l\pi}\hat{F}_{20}, & n_0 \neq 0, n = 0, \\ \frac{1}{2l\pi}\hat{F}_{20}, & n_0 \neq 0, n = 2n_0, \\ \frac{1}{l\pi}\hat{F}_{20}, & n_0 = 0, n = 0, \\ 0, & \text{other,} \end{cases} \quad \langle \tilde{F}_{11}, \beta_n \rangle = \begin{cases} \frac{1}{l\pi}\hat{F}_{11}, & n_0 \neq 0, n = 0, \\ \frac{1}{2l\pi}\hat{F}_{11}, & n_0 \neq 0, n = 2n_0, \\ \frac{1}{l\pi}\hat{F}_{11}, & n_0 = 0, n = 0, \\ 0, & \text{other,} \end{cases}$$

and  $\hat{F}_{20} = 2(\varsigma_1, \varsigma_2)^T$ ,  $\hat{F}_{11} = 2(\varrho_1, \varrho_2)^T$ .

Therefore, we can get

$$\begin{aligned}c_1(0) &= \frac{i}{2\omega_{n_0}\tilde{\tau}}(g_{20}g_{11} - 2|g_{11}|^2 - \frac{|g_{02}|^2}{3}) + \frac{1}{2}g_{21}, \quad \mu_2 = -\frac{\text{Re}(c_1(0))}{\text{Re}(\lambda'(\tilde{\tau}))}, \\ T_2 &= -\frac{1}{\omega_{n_0}\tilde{\tau}}[\text{Im}(c_1(0)) + \mu_2\text{Im}(\lambda'(\tau_n^j))], \quad \beta_2 = 2\text{Re}(c_1(0)).\end{aligned}\tag{3.13}$$

**Theorem 3.1.** For any critical value  $\tau_n^{j\pm}$  ( $n \in \mathbb{S}$ ,  $j \in \mathbb{N}$ ), we have the following results:

- (1) When  $\mu_2 > 0$  (resp.  $< 0$ ), the Hopf bifurcation is forward (resp. backward).
- (2) When  $\beta_2 < 0$  (resp.  $> 0$ ), the bifurcating periodic solutions on the center manifold are orbitally asymptotically stable (resp. unstable).
- (3) When  $T_2 > 0$  (resp.  $< 0$ ), the period increases (resp. decreases).

#### 4. Numerical simulations

For the model (1.3), we select the parameters

$$r = 0.2, \alpha = 0.8, \beta = 0.3, \mu = 0.02, \gamma = 0.06, K = 100. d_1 = 0.02, d_2 = 0.02, l = 3.$$

After explicit calculation, we can calculate the condition  $(H_0) : \theta < 29.998$ , then the system (1.3) has a positive equilibrium point. We choose  $\theta$  and  $\tau$  as the parameters of bifurcation. Their relationship is shown in Figure 1.

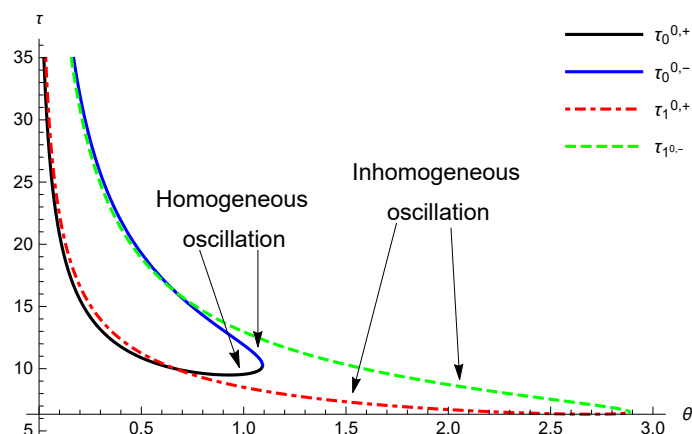


**Figure 1.** Bifurcation graph of system (1.3) with respect to  $\theta$  and  $\tau$ .

When  $\theta = 0.1$ , for system (1.3), we can figure out  $E_*(P_*, Z_*) \approx (0.3514, 0.2491)$  is a unique coexisting equilibrium, and  $\tau_0^{0,+} \approx 20.7813$ ,  $\tau_0^{0,-} \approx 45.8703$ ,  $\tau_1^{0,+} \approx 22.3497$ ,  $\tau_1^{0,-} \approx 44.2544$ . We have  $\tau_* = \tau_0^{0,+} \approx 20.7813$ ,  $\tau_{max} = \tau_0^{0,-} \approx 45.8703$ . From Theorem 2.4, it is easy to see that when  $\tau \in [0, \tau_*)$ ,  $E_*(P_*, Z_*)$  is locally asymptotically stable (shown in Figure 2). Hopf bifurcation occurs when  $\tau = \tau_*$ . When  $\tau_* < \tau < \tau_{max}$ , the system (1.3) will produce homogeneous periodic solution (shown in Figures 3–5). When  $\tau > \tau_{max}$ , We can see that the positive equilibrium point  $E_*(P_*, Z_*)$  is locally asymptotically stable (shown in Figure 6).

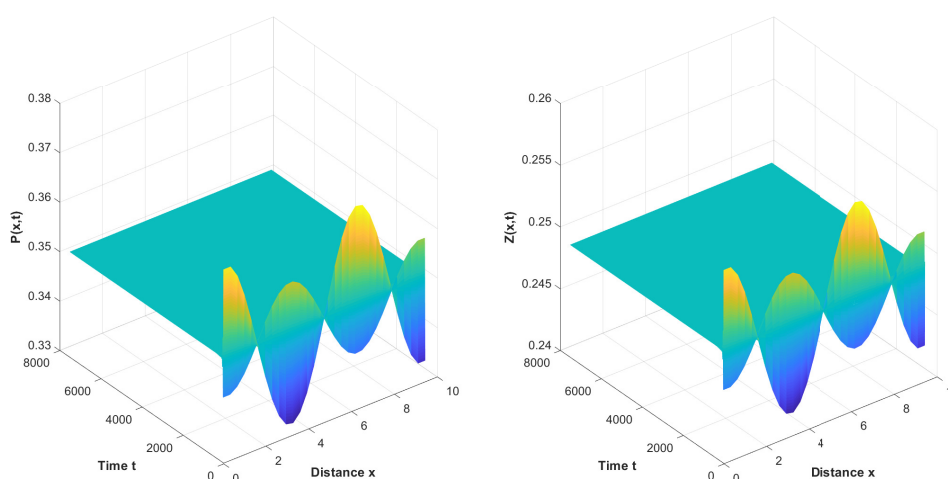
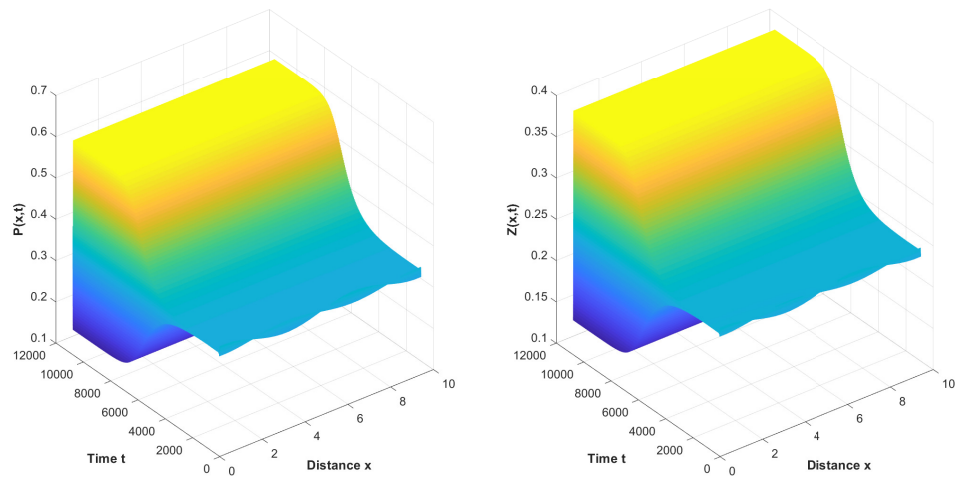
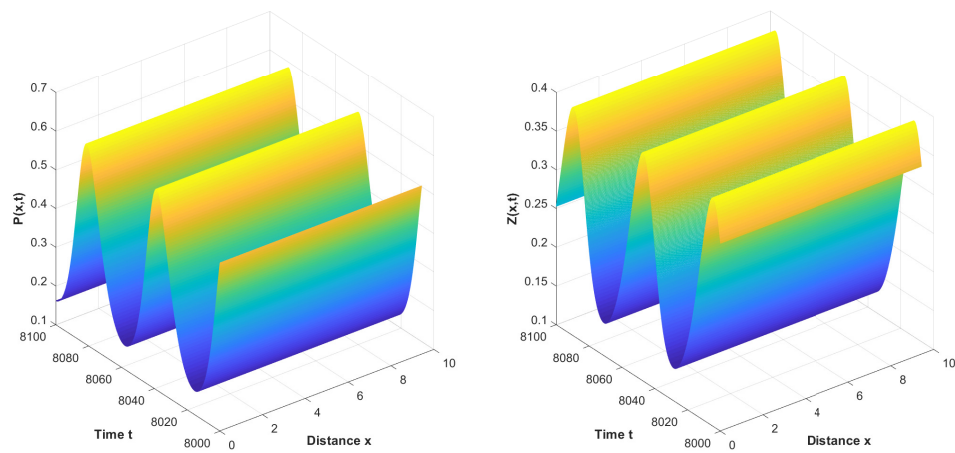


**Figure 2.** For system (1.3),  $\tau = 15$ ,  $\theta = 0.1$ ,  $E_*(P_*, Z_*) \approx (0.3514, 0.2491)$  is stable and initial condition is  $(P_* + 0.01\cos x, Z_* - 0.01\cos x)$ .

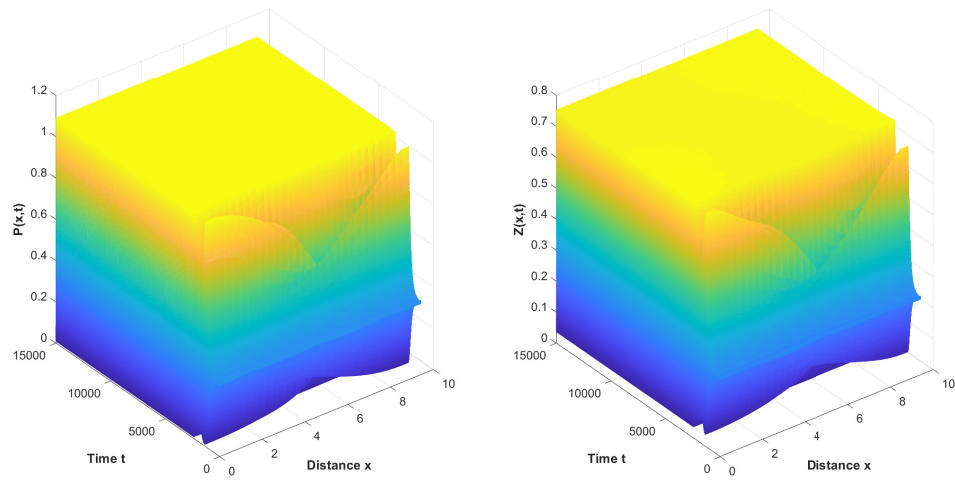


(a)

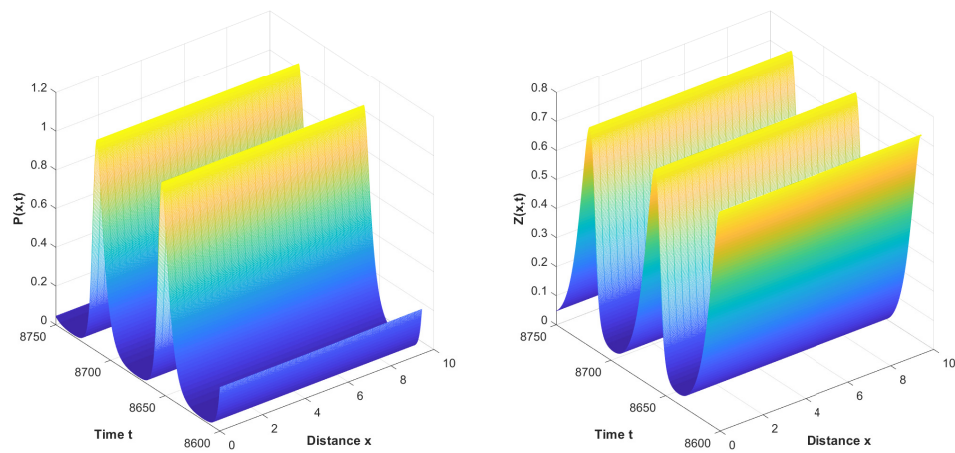


(b)

**Figure 3.** For system (1.3),  $\tau = 21.5$ ,  $\theta = 0.1$ ,  $E_*(P_*, Z_*) \approx (0.3514, 0.2491)$  is unstable and there exist spatially homogeneous periodic solution, (b) are the respective long-term behaviour of  $P(x, t)$  and  $Z(x, t)$ . In (a), initial condition is  $(P_* + 0.01\cos x, Z_* - 0.01\cos x)$ .

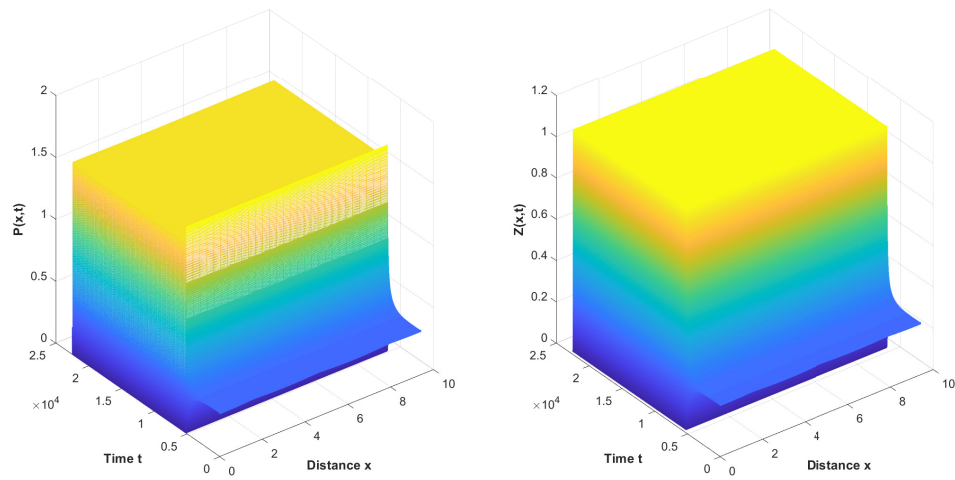


(c)

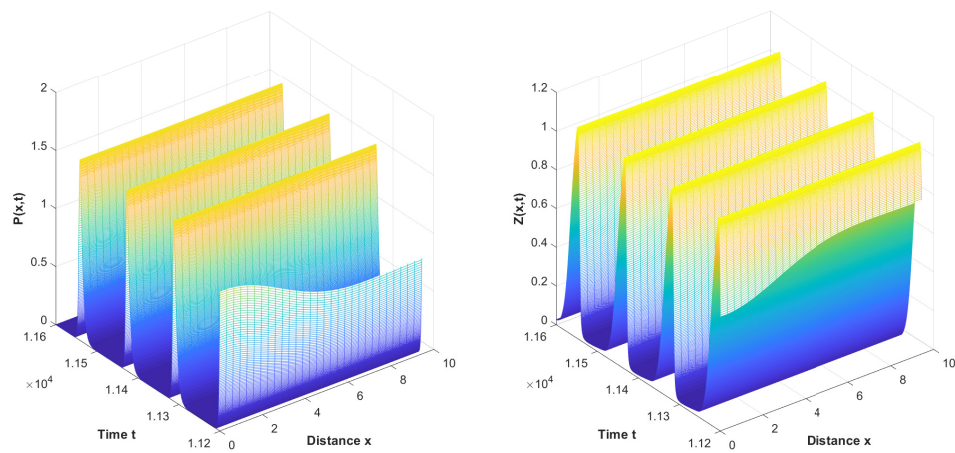


(d)

**Figure 4.** For system (1.3),  $\tau = 30$ ,  $\theta = 0.1$ ,  $E_*(P_*, Z_*) \approx (0.3514, 0.2491)$  is unstable and there exist spatially homogeneous periodic solution, (d) are the respective long-term behaviour of  $P(x, t)$  and  $Z(x, t)$ . In (c), initial condition is  $(P_* + 0.01\cos x, Z_* - 0.01\cos x)$ .



(e)



(f)

**Figure 5.** For system (1.3),  $\tau = 45$ ,  $\theta = 0.1$ ,  $E_*(P_*, Z_*) \approx (0.3514, 0.2491)$  is unstable and there exist spatially homogeneous periodic solution, (f) are the respective long-term behaviour of  $P(x, t)$  and  $Z(x, t)$ . In (e), initial condition is  $(P_* + 0.01\cos x, Z_* - 0.01\cos x)$ .

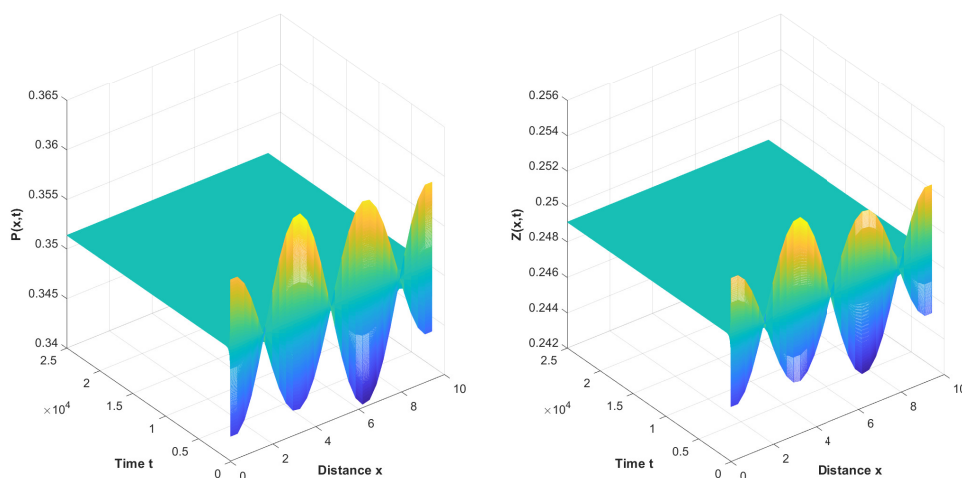


**Figure 6.** For system (1.3),  $\tau = 50$ ,  $\theta = 0.1$ ,  $E_*(P_*, Z_*) \approx (0.3514, 0.2491)$  is stable and initial condition is  $(P_* + 0.01\cos x, Z_* - 0.01\cos x)$ .

If  $\theta = 1$ , for system (1.3), we can figure out that  $E_*(P_*, Z_*) \approx (3.3412, 0.2417)$  is the unique coexisting equilibrium. Through accurate calculation,  $\tau_0^{0,+} \approx 9.5497$ ,  $\tau_0^{0,-} \approx 11.9063$ ,  $\tau_1^{0,+} \approx 8.5056$ ,  $\tau_1^{0,-} \approx 12.9598$ . Obviously to see  $\tau_* = \tau_1^{0,+} \approx 8.5056$  and  $\tau_{max} = \tau_1^{0,-} \approx 12.9598$ . According to the content in the Theorem 2.4, we know that  $E_*(P_*, Z_*)$  is locally asymptotically stable when  $\tau \in [0, \tau_*)$  (shown in Figure 7). Hopf bifurcation occurs when  $\tau = \tau_*$ . By Theorem 3.1, we can calculate that

$$\mu_2 \approx 1.9121 > 0, \quad \beta_2 \approx -0.005 < 0, \quad T_2 \approx 0.0127 > 0.$$

Hence, if  $\tau_* < \tau < \tau_{max}$ , there is a stably spatially inhomogeneous bifurcation periodic solution (showed in Figures 8–10). If  $\tau > \tau_{max}$ , we can see that  $E_*(P_*, Z_*)$  is locally asymptotically stable for the system (1.3) (showed in Figure 11).

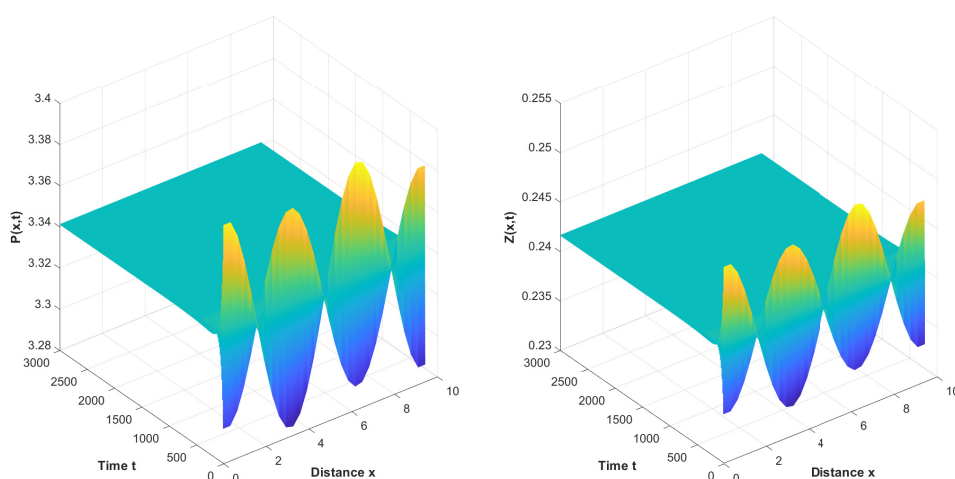
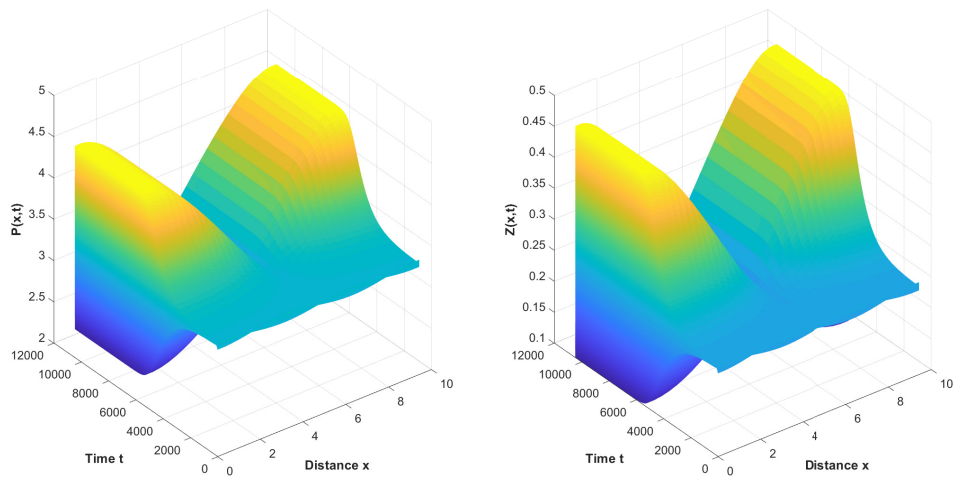
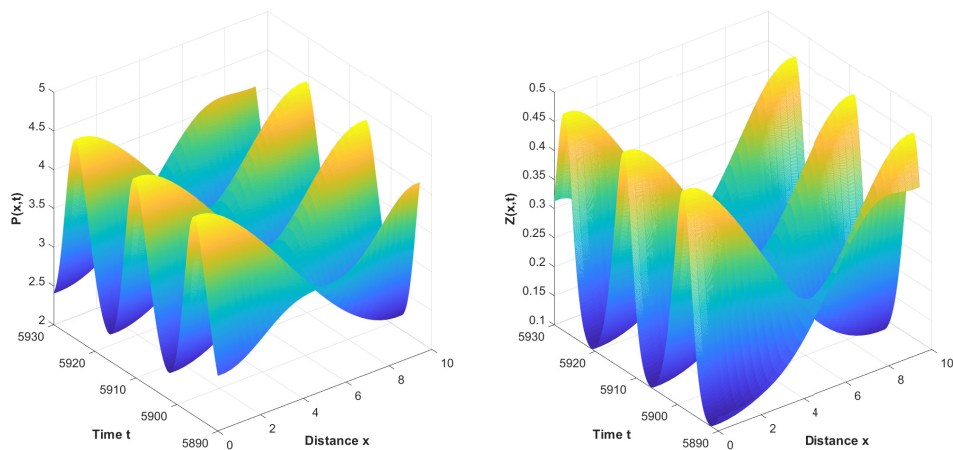


**Figure 7.** For system (1.3),  $\tau = 6$ ,  $\theta = 1$ ,  $E_*(P_*, Z_*) \approx (3.3412, 0.2417)$  is stable and initial condition is  $(P_* + 0.01\cos x, Z_* - 0.01\cos x)$ .

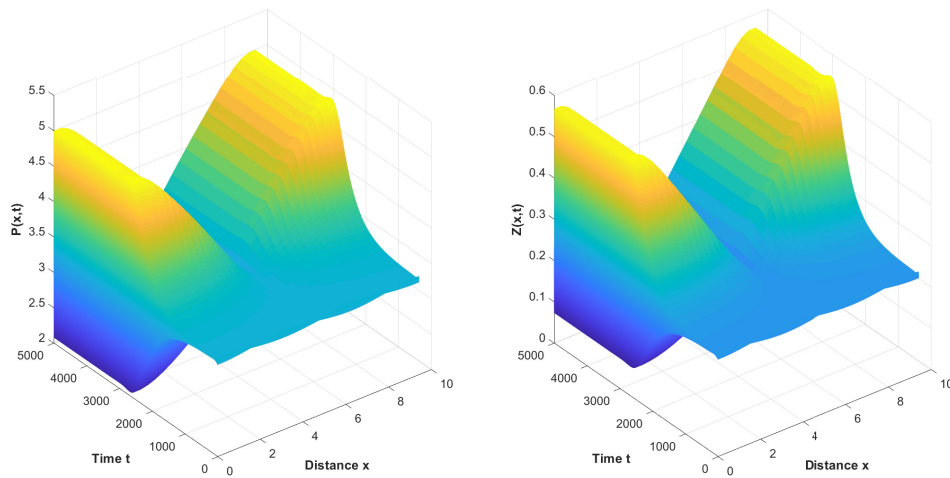


(g)

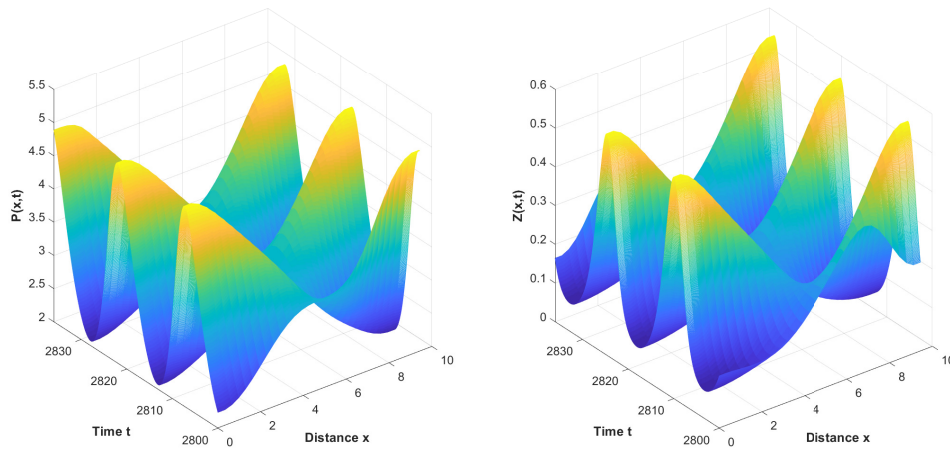


(h)

**Figure 8.** For system (1.3),  $\tau = 8.7$ ,  $\theta = 1$ ,  $E_*(P_*, Z_*) \approx (3.3412, 0.2417)$  is unstable and there exist spatially inhomogeneous periodic solution, (h) are the respective long-term behaviour of  $P(x, t)$  and  $Z(x, t)$ . In (g), initial condition is  $(P_* + 0.01\cos x, Z_* - 0.01\cos x)$ .

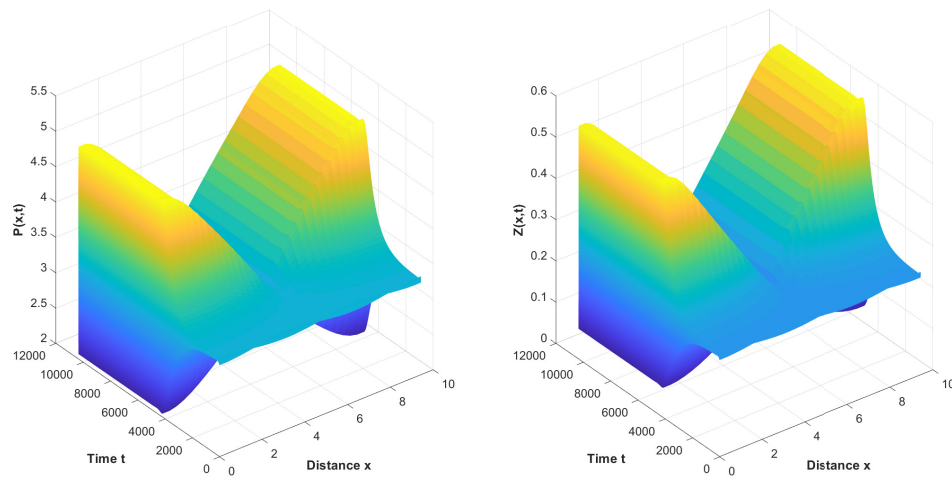


(l)

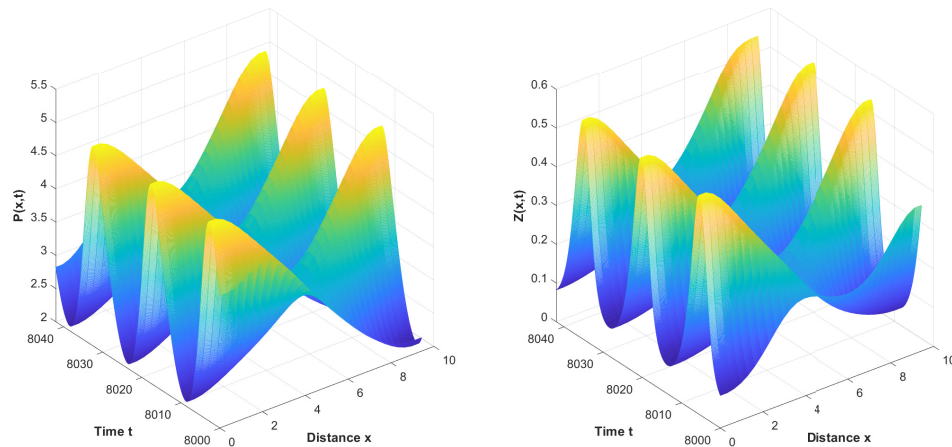


(m)

**Figure 9.** For system (1.3),  $\tau = 10, \theta = 1, E_*(P_*, Z_*) \approx (3.3412, 0.2417)$  is unstable and there exist spatially inhomogeneous periodic solution, (m) are the respective long-term behaviour of  $P(x, t)$  and  $Z(x, t)$  and  $Z_*$ . In (l), initial condition is  $(P_* + 0.01\cos x, Z_* - 0.01\cos x)$ .



(n)



(o)

**Figure 10.** For system (1.3),  $\tau = 12.9$ ,  $\theta = 1$ ,  $E_*(P_*, Z_*) \approx (3.3412, 0.2417)$  is unstable and there exist spatially inhomogeneous periodic solution, (o) are the respective long-term behaviour of  $P(x, t)$  and  $Z(x, t)$ . In (n), initial condition is  $(P_* + 0.01\cos x, Z_* - 0.01\cos x)$ .

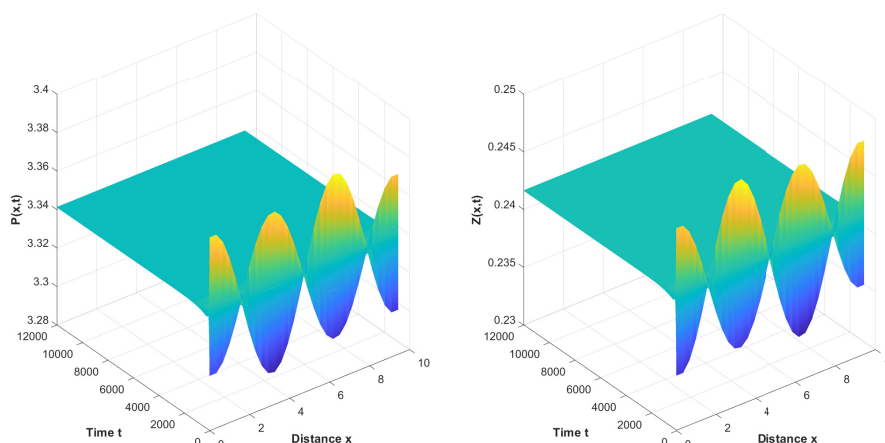


**Figure 11.** For system (1.3),  $\tau = 15$ ,  $\theta = 1$ ,  $E_*(P_*, Z_*) \approx (3.3412, 0.2417)$  is stable and initial condition is  $(P_* + 0.01\cos x, Z_* - 0.01\cos x)$ .

As a comparison, for system (1.2) without nonlocal competition, we choose the same parameters and  $\tau$ . In this case, the system (1.2) only has homogeneous stable periodic solution, which we can get  $\tau_0^{0,+} \approx 9.5497$ ,  $\tau_0^{0,-} \approx 11.9063$ . Then  $\tau_* = \tau_0^{0,+} \approx 9.5497$  and  $\tau_{max} = \tau_0^{0,-} \approx 11.9063$ . From Theorem 2.4, it is clear that if  $\tau \in [0, \tau_*)$ ,  $E_*(P_*, Z_*)$  is locally asymptotically stable (shown in Figures 12 and 13). For the system (1.2) the Hopf bifurcation occurs when  $\tau = \tau_*$ . Thus, there is a stably spatially homogeneous bifurcation periodic solution when  $\tau_* < \tau < \tau_{max}$  (showed in Figure 14). If  $\tau > \tau_{max}$ , we can see that  $E_*(P_*, Z_*)$  is locally asymptotically stable (showed in Figures 15 and 16).

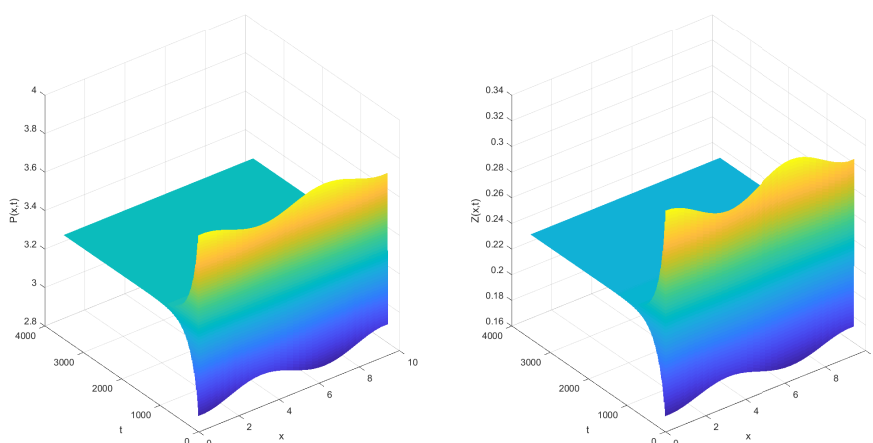


**Figure 12.** For system (1.2),  $\tau = 6$ ,  $\theta = 1$ ,  $E_*(P_*, Z_*) \approx (3.3412, 0.2417)$  is stable and initial condition is  $(P_* + 0.01\cos x, Z_* - 0.01\cos x)$ .

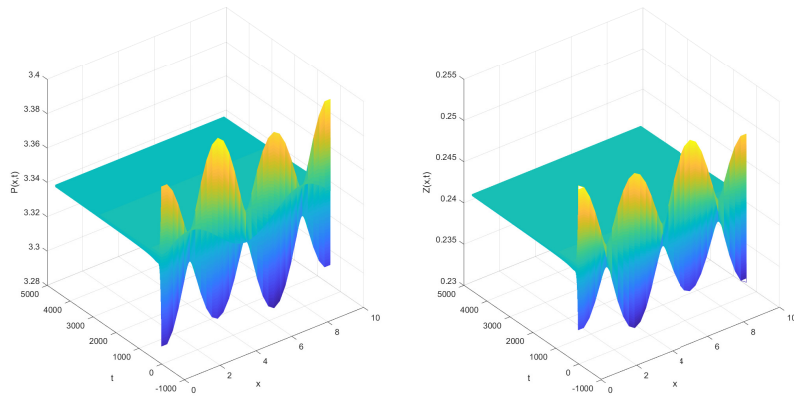
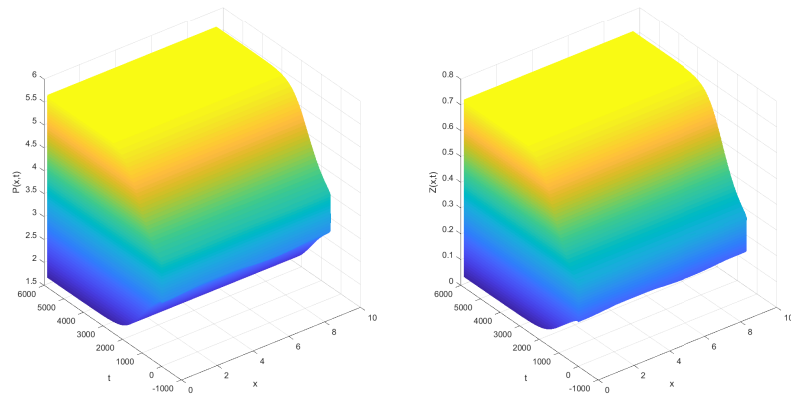
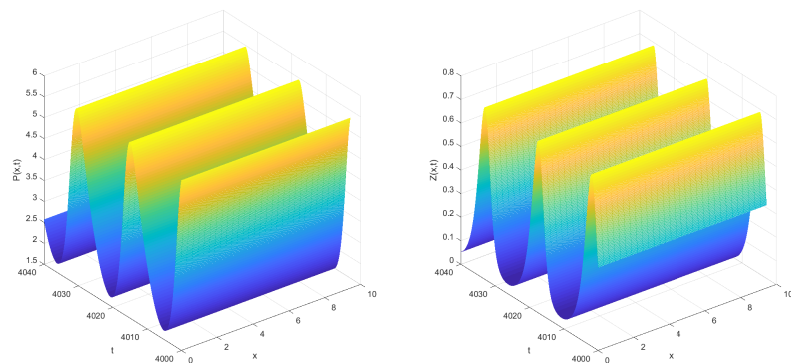


**Figure 13.** For system (1.2),  $\tau = 8.7$ ,  $\theta = 1$ ,  $E_*(P_*, Z_*) \approx (3.3412, 0.2417)$  is stable and initial condition is  $(P_* + 0.01\cos x, Z_* - 0.01\cos x)$ .



(p)



(q)

**Figure 14.** For system (1.2),  $\tau = 10$ ,  $\theta = 1$ ,  $E_*(P_*, Z_*) \approx (3.3412, 0.2417)$  is unstable and there exist spatially homogeneous periodic solution, (q) are the respective long-term behaviour of  $P(x, t)$  and  $Z(x, t)$ . In (p), initial condition is  $(P_* + 0.01\cos x, Z_* - 0.01\cos x)$ .

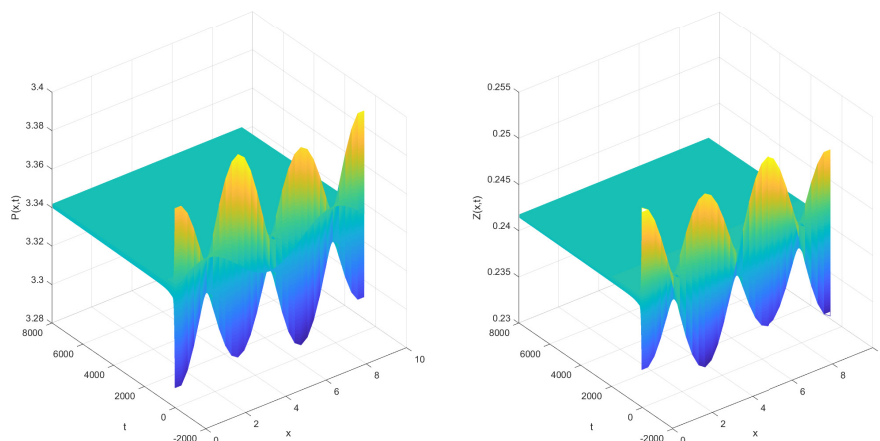


**Figure 15.** For system (1.2),  $\tau = 12.9$ ,  $\theta = 1$ ,  $E_*(P_*, Z_*) \approx (3.3412, 0.2417)$  is stable and initial condition is  $(P_* + 0.01\cos x, Z_* - 0.01\cos x)$ .

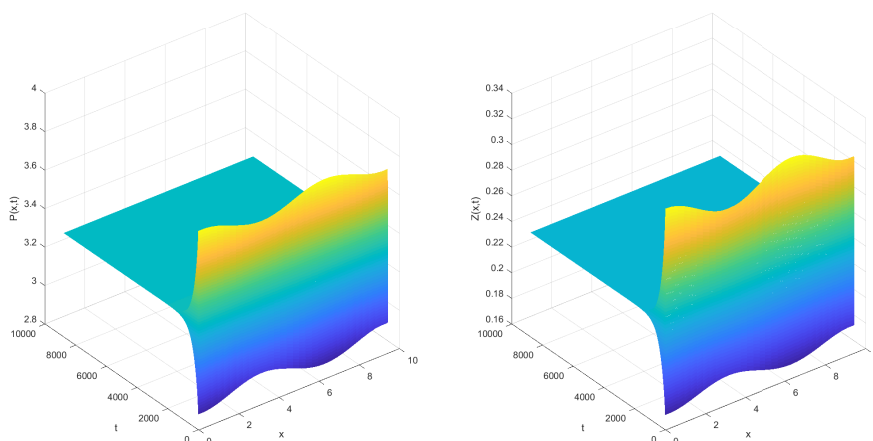


**Figure 16.** For system (1.2),  $\tau = 15$ ,  $\theta = 1$ ,  $E_*(P_*, Z_*) \approx (3.3412, 0.2417)$  is stable and initial condition is  $(P_* + 0.01\cos x, Z_* - 0.01\cos x)$ .

If  $\theta = 1.5$ , for system (1.3), it can be seen from the Figure 1 that the system (1.3) has inhomogeneous stable periodic solution. After precise calculation, we can get the unique coexisting equilibrium is  $E_*(P_*, Z_*) \approx (5.0075, 0.2374)$ . We can calculate that  $\tau_1^{0,+} \approx 7.3418$ ,  $\tau_1^{0,-} \approx 10.3281$ , we have  $\tau_* = \tau_1^{0,+} \approx 7.3418$  and  $\tau_{max} = \tau_1^{0,-} \approx 10.3281$ . From Theorem 2.4, it is clear that if  $\tau \in [0, \tau_*)$ ,  $E_*(P_*, Z_*)$  is locally asymptotically stable (shown in Figure 17). Hopf bifurcation occurs when  $\tau = \tau_*$ . There is a stably spatially inhomogeneous bifurcating periodic solution when  $\tau_* < \tau < \tau_{max}$  (shown in Figure 18). In addition, for the system (1.3),  $E_*(P_*, Z_*)$  is locally asymptotically stable when  $\tau > \tau_{max}$  (shown in Figure 19).

**Remark:** In this section, the Figure 1 was drawn using Wolfram Mathematica and the other images were drawn using Matlab.

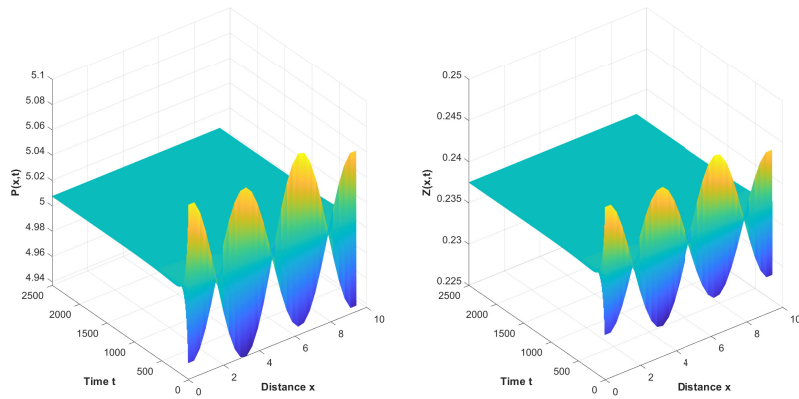
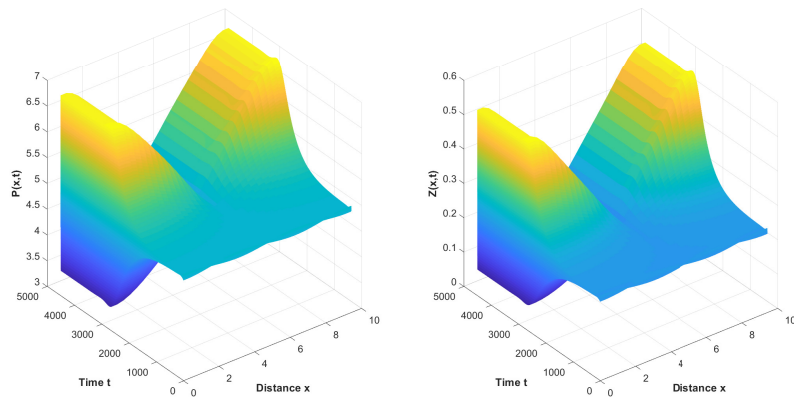
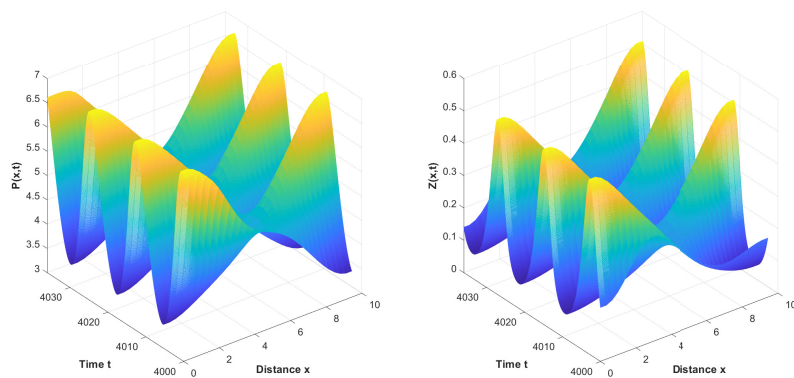


**Figure 17.** For system (1.3),  $\tau = 5, \theta = 1.5, E_*(P_*, Z_*) \approx (5.0075, 0.2374)$  is stable and initial condition is  $(P_* + 0.01\cos x, Z_* - 0.01\cos x)$ .



(r)



(s)

**Figure 18.** For system (1.3),  $\tau = 9, \theta = 1.5, E_*(P_*, Z_*) \approx (5.0075, 0.2374)$  is unstable and there exist spatially inhomogeneous periodic solution, (s) are the respective long-term behaviour of  $P(x, t)$  and  $Z(x, t)$ . In (r), initial condition is  $(P_* + 0.01\cos x, Z_* - 0.01\cos x)$ .

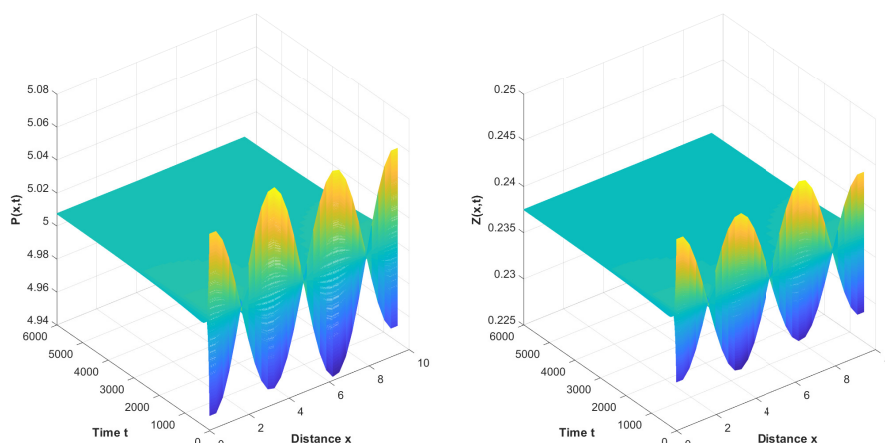


**Figure 19.** For system (1.3),  $\tau = 12$ ,  $\theta = 1.5$ ,  $E_*(P_*, Z_*) \approx (5.0075, 0.2374)$  is stable and initial condition is  $(P_* + 0.01\cos x, Z_* - 0.01\cos x)$ .

## 5. Conclusions

In this paper, a delayed diffusive plankton model with nonlocal competition is deeply studied by us. We mainly study the local stability of coexisting equilibrium and existence of Hopf bifurcations. Through the normal form method and center manifold theorem, we also analysis the property of bifurcating periodic solution.

Making the rate of phytoplankton toxin production as an important parameter, it can be seen from Figure 1 in the numerical simulation, as  $\theta$  increase, the stability critical value of the system (1.3) decreases gradually, and when the rate of toxins produced by each kind of phytoplankton is in a certain range, the system (1.3) changes from homogeneous periodic solution to inhomogeneous periodic solution. In real life, the distribution of phytoplankton and zooplankton always present the inhomogeneous state, so in order to better fit the actual situation, we choose to focus on the analysis of the inhomogeneous parts. The image of the fourth part is also displayed that with the increase of  $\tau$ , the system (1.3) exists a stability switch, presents a process from stable to inhomogeneous solution and then to stable, which also explicates that when the rate of phytoplankton producing toxins is fixed, the bigger the value of  $\tau$ , the more conducive to the stability of the plankton population. And compared with the model (1.3) with the nonlocal competition term, the system (1.2) without the nonlocal competition also has the same steady state solution, and there is also a stability switch as  $\tau$  increases. However, only homogeneous periodic solution can be found, which explains that the stably spatial inhomogeneous periodic solution exists only when the nonlocal competitive term and the diffusive term exist simultaneously, the introduction of nonlocal competitive term makes the dynamic behavior of the model more sophisticated, but also more realistic.

Future research direction: The study of the fractional-order dynamical models is also interesting. In [25], their results are of great significance to the design of neural networks, and the bifurcation theory of fractional order delay differential equations are greatly enriched. We will take the Hopf bifurcation of fractional-order dynamical models as the future research direction.

## Funding

This research is supported by the Fundamental Research Funds for the Central Universities (Grant No. 2572022DJ04).

## Author contributions

All authors contributed to the study conception and design. Material preparation, data collection and analysis were performed by Liye Wang. All authors read and approved the final manuscript.

## Data availability

Data sharing is not applicable to this article as no datasets were generated or analyzed during the current study.

## Conflict of interest

The authors have no relevant financial or non-financial interests to disclose.

## References

1. R. Pal, D. Basu, M. Banerjee, Modelling of phytoplankton allelopathy with Monod-Haldane-type functional response-A mathematical study, *Biosystems*, **95** (2009), 243–253. <https://doi.org/10.1016/j.biosystems.2008.11.002>
2. S. Chakraborty, P. K. Tiwari, A. K. Misra, J. Chattopadhyay, Spatial dynamics of a nutrient-phytoplankton system with toxic effect on phytoplankton, *Math. Biosci.*, **264** (2015), 94–100. <https://doi.org/10.1016/j.mbs.2015.03.010>
3. X. Y. Meng, Y. Q. Wu, Dynamical analysis of a fuzzy phytoplankton-zooplankton model with refuge, fishery protection and harvesting, *J. Appl. Math. Comput.*, **63** (2020), 361–389. <http://doi.org/10.1007/s12190-020-01321-y>
4. F. Zhang, J. Sun, W. Tian, Spatiotemporal pattern selection in a nontoxic-phytoplankton-toxic-phytoplankton-zooplankton model with toxin avoidance effects, *Appl. Math. Comput.*, **423** (2022), 127007. <https://doi.org/10.1016/j.amc.2022.127007>
5. T. Zhang, W. Wang, Hopf bifurcation and bistability of a nutrient-phytoplankton-zooplankton model, *Appl. Math. Model.*, **36** (2012), 6225–6235. <https://doi.org/10.1016/j.apm.2012.02.012>
6. A. Mondal, S. Mondal, S. Mandal, Empirical dynamic model deciphers more information on the nutrient (N)-phytoplankton (P)-zooplankton (Z) dynamics of Hooghly-Matla estuary, Sundarban, India. *Estuar. Coast. Shelf Sci.*, **265** (2022), 107711. <https://doi.org/10.1016/j.ecss.2021.107711>
7. F. Zhang, W. Zhou, L. Yao, X. Wu, H. Zhang, Spatiotemporal patterns formed by a discrete Nutrient-Phytoplankton model with time delay, *Complexity*, **2020** (2020), 8541432. <https://doi.org/10.1155/2020/8541432>

8. K. Zhuang, Y. Li, B. Gong, Stability switches and Hopf bifurcation induced by nutrient recycling delay in a reaction-diffusion nutrient-phytoplankton model, *Complexity*, **2021** (2021), 7943788. <https://doi.org/10.1155/2021/7943788>
9. R. Yang, D. Jin, W. Wang, A diffusive predator-prey model with generalist predator and time delay, *AIMS Mathematics*, **7** (2022), 4574–4591. <https://doi.org/10.3934/math.2022255>
10. R. Yang, X. Zhao, Y. An, Dynamical analysis of a delayed diffusive predator-prey model with additional food provided and anti-predator behavior, *Mathematics*, **10** (2022), 469. <https://doi.org/10.3390/math10030469>
11. R. Yang, Q. Song, Y. An, Spatiotemporal dynamics in a predator-prey model with functional response increasing in both predator and prey densities, *Mathematics*, **10** (2022), 17. <https://doi.org/10.3390/math10010017>
12. J. Chattopadhyay, R. R. Sarkar, A. E. Abdllaoui, A delay differential equation model on harmful algal blooms in the presence of toxic substances, *Math. Med. Biol.*, **19** (2002), 137–161. <https://doi.org/10.1093/imammb/19.2.137>
13. J. Zhao, J. Wei, Dynamics in a diffusive plankton system with delay and toxic substances effect, *Nonlinear Anal. Real World Appl.*, **22** (2015), 66–83. <https://doi.org/10.1016/j.nonrwa.2014.07.010>
14. N. F. Britton, Aggregation and the competitive exclusion principle, *J. Theor. Biol.*, **136** (1989), 57–66. [https://doi.org/10.1016/S0022-5193\(89\)80189-4](https://doi.org/10.1016/S0022-5193(89)80189-4)
15. J. Furter, M. Grinfeld, Local vs. non-local interactions in population dynamics, *J. Math. Biol.*, **27** (1989), 65–80. <https://doi.org/10.1007/BF00276081>
16. D. Geng, W. Jiang, Y. Lou, H. Wang, Spatiotemporal patterns in a diffusive predator-prey system with nonlocal intraspecific prey competition, *Stud. Appl. Math.*, **148** (2022), 396–432. <https://doi.org/10.1111/sapm.12444>
17. S. Pal, S. Petrovskii, S. Ghorai, M. Banerjee, Spatiotemporal pattern formation in 2D prey-predator system with nonlocal intraspecific competition, *Commun. Nonlinear Sci. Numer. Simul.*, **93** (2021), 105478. <https://doi.org/10.1016/j.cnsns.2020.105478>
18. M. K. Pal, S. Poria, Effects of non-local competition on plankton-fish dynamics, *Chaos*, **31** (2021), 053108. <https://doi.org/10.1063/5.0040844>
19. S. Wu, Y. Song, Stability and spatiotemporal dynamics in a diffusive predator-prey model with nonlocal prey competition, *Nonlinear Anal. Real World Appl.*, **48** (2019), 12–39. <https://doi.org/10.1016/j.nonrwa.2019.01.004>
20. R. Yang, C. Nie, D. Jin, Spatiotemporal dynamics induced by nonlocal competition in a diffusive predator-prey system with habitat complexity, *Nonlinear Dyn.*, **110** (2022), 879–900. <https://doi.org/10.1007/s11071-022-07625-x>
21. R. Yang, F. Wang, D. Jin, Spatially inhomogeneous bifurcating periodic solutions induced by nonlocal competition in a predator-prey system with additional food, *Math. Methods Appl. Sci.*, **45** (2022), 9967–9978. <https://doi.org/10.1002/mma.8349>
22. S. Chen, J. Shi, Stability and Hopf bifurcation in a diffusive logistic population model with nonlocal delay effect, *J. Differ. Equ.*, **253** (2012), 3440–3470. <https://doi.org/10.1016/j.jde.2012.08.031>

- 
23. J. Wu, *Theory and Applications of Partial Functional Differential Equations*, New York: Springer, 1996. <https://doi.org/10.1007/978-1-4612-4050-1>
  24. B. D. Hassard, N. D. Kazarinoff, Y. H. Wan, *Theory and Applications of Hopf Bifurcation*, Cambridge: Cambridge University Press, 1981. <http://doi.org/10.1090/conm/445>
  25. C. Xu, M. Liao, P. Li, Y. Guo, Z. Liu, Bifurcation properties for fractional order delayed BAM neural networks, *Cognit. Comput.*, **13** (2021), 322–356. <https://doi.org/10.1007/s12559-020-09782-w>



AIMS Press

©2023 the Author(s), licensee AIMS Press. This is an open access article distributed under the terms of the Creative Commons Attribution License (<http://creativecommons.org/licenses/by/4.0>)